Magnetically Induced Electronic Ferroelectricity in Half-Doped Manganites

Gianluca Giovannetti,[1,2,5] Sanjeev Kumar,[1,2] Jeroen van den Brink,[1,3,4] and Silvia Picozzi[5]

[1]*Institute Lorentz for Theoretical Physics, Leiden University, Leiden, The Netherlands*
[2]*Faculty of Science and Technology and MESA+ Research Institute, University of Twente, Enschede, The Netherlands*
[3]*Stanford Institute for Materials and Energy Sciences, Stanford University and SLAC National Accelerator Laboratory, Menlo Park, California 94025, USA*
[4]*Institute for Molecules and Materials, Radboud Universiteit, Nijmegen, The Netherlands*
[5]*Consiglio Nazionale delle Ricerche–Istituto Nazionale per la Fisica della Materia (CNR-INFM), CASTI Regional Laboratory, 67100 L'Aquila, Italy*

(Received 23 December 2008; published 17 July 2009)

Using a joint approach of density functional theory and model calculations, we demonstrate that a prototypical charge ordered half-doped manganite $La_{1/2}Ca_{1/2}MnO_3$ is multiferroic. The combination of a peculiar charge-orbital ordering and a tendency to form spin dimers breaks the inversion symmetry and leads to a ferroelectric ground state with a polarization up to several $\mu C/cm^2$. The presence of improper ferroelectricity does not depend on the hotly debated structural details of this material: in the Zener-polaron structure we find a similar ferroelectric response with a large polarization of purely magnetic origin.

DOI: 10.1103/PhysRevLett.103.037601 PACS numbers: 77.80.−e, 71.15.Mb, 75.47.Lx

Materials with simultaneous magnetic and ferroelectric ordering—multiferroics—are attracting enormous scientific interest [1,2]. They offer the potential to control magnetic properties by electric fields and, vice versa, ferroelectric order by magnetic fields—a very desirable property from a technological point of view [3]. Such control requires large multiferroic couplings: a substantial ferroelectric polarization needs to be induced by the magnetic ordering. Even if in quite a few materials ferroelectricity and magnetism coexist, multiferroic couplings appear to be tiny [4–6]. When designing materials with large multiferroic couplings, one has to exclude from the start the largest class of multiferroics, the ones in which multiferroicity is driven by spiral magnetic ordering. In these materials multiferroicity relies on relativistic spin-orbit coupling as a driving force, which is intrinsically weak [1]. Charge ordered magnetic compounds are a far more promising class of materials with potentially large multiferroic couplings [7]. The coexistence of charge ordering and magnetism is found in a substantial number of transition metal oxides, e.g., ferrites, nickelates, and cobaltates [8]. To become strongly multiferroic such a material needs to meet three additional requirements: (i) the symmetry is such that the magnetic ordering can push the charge ordering pattern from site-centered (SC) to bond-centered (BC) or vice versa [9], (ii) the material is insulating, as it has to support a ferroelectric polarization, and (iii) the material is electronically soft, so that inside it charge can easily be displaced. Half-doped manganites of the type $La_{1/2}Ca_{1/2}MnO_3$ famously meet the last two requirements [10]. Here we show it also fulfills the first one, so that a strong multiferroic coupling emerges.

In a combined approach of *ab initio* density functional and model Hamiltonian calculations we show that the strong electron-electron interactions combined with the Jahn-Teller (JT) lattice distortions that are present in this manganese oxide cause a canting instability of its antiferromagnetic (AFM) ground state, driving a reconstruction of its charge ordering from site-centered towards bond-centered. The resulting noncollinear magnetic ordering induces in $La_{1/2}Ca_{1/2}MnO_3$ a purely electronic polarization of several $\mu C/cm^2$, a multiferroic coupling almost 2 orders of magnitude larger than the one of a typical multiferroic [5] such as $TbMn_2O_5$.

We consider a half-doped manganite $La_{1/2}Ca_{1/2}MnO_3$ (LCMO) in the experimentally observed antiferromagnetic CE [11,12] double-zigzag spin state [see Fig. 1(a)], which is stable below $T_N \sim 155$ K. Despite having a long history [12,13], the experimental crystallographic and corresponding electronic structure of LCMO (as that of the closely related $Pr_{1-x}Ca_xMnO_3$, $x \sim 0.5$) is still debated [14]. On one hand, a traditional checkerboard charge order (CO) state has been proposed [11], given by the alternation of orbitally ordered Mn^{3+} (at the center of Jahn-Teller distorted octahedra) and Mn^{4+} (in a largely undistorted octahedron) with a mostly SC CO. On the other hand, a BC model has been suggested [15,16], based on the so-called Zener-polaron (ZP) state where equivalent Mn d^4 ions, showing no charge disproportionation (CD), couple into ferromagnetic (FM) dimers sharing a spin-polarized hole on the intermediate O atom. In both SC and BC cases, we find magnetic ground state structures that break inversion symmetry (IS) and result in polar states with relatively strong ferroelectricity [17].

First-principles studies have proven to be tremendously helpful to shed light on the microscopic origin and on the quantitative evaluation of the electric polarization P in several improper magnetic ferroelectrics [18–21]. Our den-

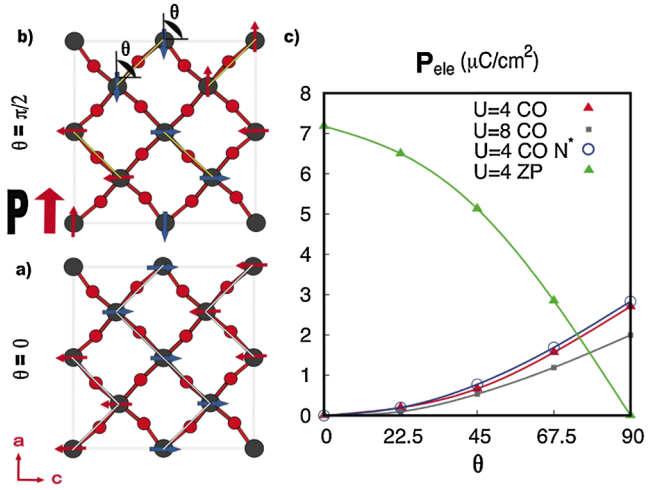

FIG. 1 (color online). Spin directions in the MnO_2 plane for (a) $\theta = 0°$ (AFM CE) and (b) $\theta = 90°$ ($\perp$). Zigzag chains and FM dimers highlighted. (c) Electronic polarization P_{ele} (in $\mu\text{C/cm}^2$) vs θ (in degrees) for $U = 4$ eV and $U = 8$ eV for the experimental ionic structure of Ref. [11] (CO) and of Ref. [27] (ZP). "Half-doping" is simulated both with (i) a checkerboard arrangement of La and Ca ions and (ii) replacing La by Ca + e^- in LCMO, while retaining the crystal structure of LCMO, and compensating with a homogeneous positive background (denoted as N^*).

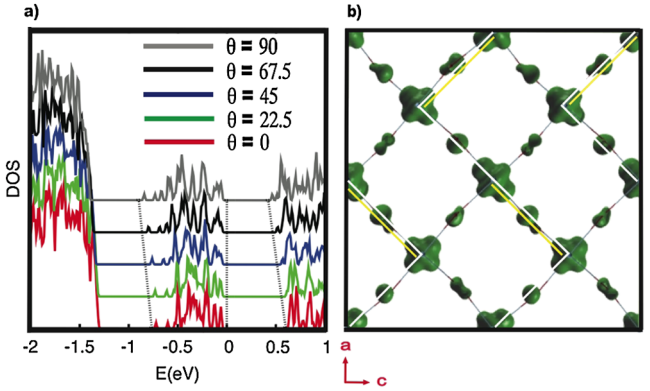

FIG. 2 (color online). DFT results. (a) Total DOS for different θ: DOS are arbitrarily shifted on the y axis with a shift proportional to θ. The zero of the energy scale marks the Fermi level. (b) Isosurface of the e_g bands in the $\perp$ structure: view on the MnO_2 plane.

sity functional theory (DFT) simulations are performed within the generalized gradient approximation (GGA) [22] to the exchange-correlation potential and treating the Mn d electrons via a Hubbard-like potential within GGA + U [23] (unless otherwise noted, $U = 4$ eV, $J = 0.9$ eV). We used the Vienna *ab initio* simulation package (VASP) [24], including the noncollinear-spin formalism [25] and the Berry-phase (BP) approach to evaluate electric polarization P [26]. The cutoff for the plane-wave basis set was chosen as 400 eV for the collinear and noncollinear spin configurations and a $[3, 3, 4]$ mesh was used for the Brillouin-zone sampling. In the BP approach, we integrated over 12 $\mathbf{k}$-space strings parallel to either the a or b axis, each string divided in 8 $\mathbf{k}$ points. The experimental lattice parameters and ionic positions were taken from Ref. [11] for the CO-like structure ($P2_1/m$ space group) and from Ref. [27] for the ZP-like structure ($P2_1nm$ space group).

From our calculations we find that the CE-type AFM [Fig. 1(a)] is insulating [see Fig. 2(a)] and clearly orbitally ordered, with a small CD, consistent with previous collinear-spin electronic-structure works [28]. For $U = 4$ eV, there is a clear gap; the CD amounts to $\delta \sim 0.15e^-$ whereas the magnetic moments are $\sim 3.3\mu_B$ and $3.05\mu_B$ on the nominally Mn^{3+} and Mn^{4+}, respectively. The BP calculation of P shows, as expected, that the centrosymmetric CE-type structure is paraelectric. However, a spin-rotation immediately induces a ferroelectric moment. We consider a rotation of the spins of two neighboring Mn (one 3+ and one 4 +) along the up spin chain by an angle θ and, correspondingly, one dimer in the down spin chain by the same angle. This particular spin rotation is motivated by the fact that it tunes the magnetic CE state continuously towards the one compatible with ZP structure (denoted as $\perp$), which corresponds to $\theta = 90°$ and is shown in Fig. 1(b). The calculated electronic polarization P_{ele} increases monotonically with θ, reaching $\sim 3\ \mu\text{C/cm}^2$ for $\theta = 90°$. Importantly, the results are stable with respect to an increase in the value of U, and the details of how the half-doping is achieved within DFT [see Fig. 1(c)].

The resulting total density of states (DOS) shows that a larger value of θ broadens the e_g band (which is about 0.7 eV wide), therefore reducing the band gap [see Fig. 2(a)]. In Fig. 2(b) we plot an isosurface of the e_g bands, indicating a clear orbital ordering (OO), with two kinds of different Mn: the nominal Mn^{3+} shows a staggered $(3x^2 - r^2)/(3y^2 - r^2)$ orbital arrangement, whereas the nominal Mn^{4+} shows a much more isotropic charge distribution, as given by partial occupation of both $(3z^2 - r^2)$ and $(x^2 - y^2)$ orbitals. Since this situation is very similar to the collinear CE case (not shown), it proves that the spin rotation alone does not alter significantly the CO/OO.

In order to investigate the stability of the CE-type AFM state with respect to the rotation of spin dimers, we study the degenerate double-exchange model in the presence of the interorbital Hubbard repulsion and JT lattice distortions, with the Hamiltonian

$$H = -\sum_{\langle ij\rangle}^{\alpha\beta} t_{\alpha\beta}^{ij} \cos(\Theta_{ij}/2) c_{i\alpha}^{\dagger} c_{j\beta} + U \sum_i n_{ia} n_{ib} + J_s \sum_{\langle ij\rangle} \mathbf{S}_i \cdot \mathbf{S}_j - \lambda \sum_i \mathbf{Q}_i \cdot \boldsymbol{\tau}_i + \frac{K}{2} \sum_i \mathbf{Q}_i^2, \quad (1)$$

where c ($c^{\dagger}$) is the annihilation (creation) operator, and α, β are summed over the two Mn-e_g orbitals $d_{x^2-y^2}(a)$ and

$d_{3z^2-r^2}(b)$. $t^{ij}_{\alpha\beta}$ denote the nearest-neighbor hopping amplitudes: $t^x_{aa} = t^y_{aa} \equiv t$, $t^x_{bb} = t^y_{bb} \equiv t/3$, $t^x_{ab} = t^x_{ba} \equiv -t/\sqrt{3}$, $t^y_{ab} = t^y_{ba} \equiv t/\sqrt{3}$. The Θ_{ij} are the angle between neighboring Mn-t_{2g} spins $\mathbf{S_i}$ and $\mathbf{S_j}$ and J_s is their AFM superexchange. λ denotes the strength of the JT coupling between the distortion $\mathbf{Q}_i = (Q_{ix}, Q_{iz})$ and the orbital pseudospin $\tau^\mu_i = \sum_{\alpha\beta} c^\dagger_{i\alpha} \Gamma^\mu_{\alpha\beta} c_{i\beta}$, where Γ^μ are the Pauli matrices. K is a measure of the lattice stiffness (set to unity). Energies are in units of t [estimated $\sim$0.2 eV from the e_g bandwidth in Fig. 2(a)]. In the absence of U, a CE state with CO/OO is found to be the ground state over a wide regime in the parameter space [29]. In the absence of λ (and for $U \geq 10$), we find that the $\perp$ state has lower energy than the CE state [see Fig. 3(a)]. Inclusion of the JT coupling leads to the stability of a state with an intermediate θ. Eventually, beyond a (U-dependent) critical value of λ, one recovers the CE state as the ground state. We note that the potential well in Fig. 3(a) is very shallow ($\sim$1 meV). The presence of JT distortions corresponds to the crystal structure of Ref. [12] consistent with Fig. 1(c).

We also find a decrease in the DOS gap [Fig. 3(b)], and a broadening of the e_g bands [Fig. 3(c)] upon increasing θ, similar to the first-principles results [see Fig. 2(a)]. This can be understood in terms of the effective hoppings arising via the double exchange factor $\cos(\Theta_{ij}/2)$. In the CE state each chain has a perfect hopping, but there is no interchain hopping. However, the spin-dimerized state allows for interchain hopping at the cost of reduced hopping within chains, leading to an overall gain by a factor $(1 + \sqrt{2})/2$, which very well explains the increase in the bandwidth W [Fig. 3(c)].

Let us now focus on the multiferroicity. The creation of noncollinear "spin dimers" along with the small but detectable CD breaks IS (present in the CE spin arrangement), allowing ferroelectric (FE) polarization along the a axis as a realization of the intermediate BC/SC CO picture proposed by Efremov *et al.* [9]. There is, however, one important difference between our work and those model predictions [9]: there, the spin rotation is sufficient to progressively transform a SC-CO into a BC-CO (ZP) and, as such, the $\perp$ structure regains centrosymmetry (i.e., leading to the expectation of $P_{\rm ele} = 0$). In our case, the spin rotation—even for the largest $\theta = 90°$—is not a strong enough factor to produce a BC situation, due to the structural inequivalency between the two kinds of Mn which governs their charge distribution. Indeed, in our DFT simulations, the larger the deviation from the collinear CE type, the stronger the "asymmetry" introduced by the spin dimers along the chain and the closer one gets to the ideal realization of the intermediate BC/SC situation, explaining why the maximum is located at $\theta = 90°$. According to this mechanism, CD is an essential ingredient in the rising of P: there would be no ferroelectricity without CD (despite Mn cations keeping a centrosymmetric distribution). Rather, it is the *combination of spin-rotation and CO* that induces ferroelectricity.

We now discuss multiferroicity in an alternative lattice structure characterized by a *structural* Mn-Mn dimerization. In particular, Rodriguez *et al.* [27] proposed two different LCMO structures (referred to in that paper as LT-M and LT-O): the LT-M shows basically the same configuration and symmetries as that discussed so far (Ref. [11]), whereas the LT-O shows neighboring octahedra in which both Mn are off-centered and with "long" MnO bonds directed along the same Mn-O-Mn line. This is characteristic of a BC-CO ZP-like structure [15], in which the two Mn (despite being still inequivalent by symmetry) are electronically more similar than in the SC CO/OO model. Indeed, when plotting the LT-O isosurface for the e_g manifold [see Fig. 4(a)], the two kinds of Mn show a very similar charge distribution, as also confirmed by the small difference ($\sim 0.1 \mu_B$) between their moments. In Fig. 4(a), the peculiar OO shows *pairs* of Mn with $3x^2 - r^2$ orbitals alternated with pairs of Mn with $3y^2 - r^2$ orbitals, in agreement with the ZP picture. We do not find an appreciable spin polarization on the O in the

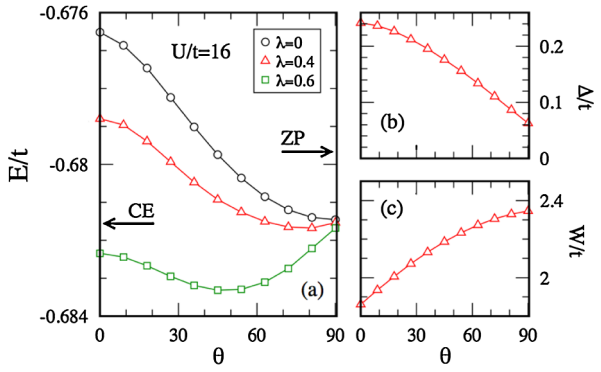

FIG. 3 (color online). Model Hamiltonian results. (a) Total energy E vs θ for different values of λ. The θ dependence of (b) DOS gap Δ and (c) the bandwidth W of the occupied e_g.

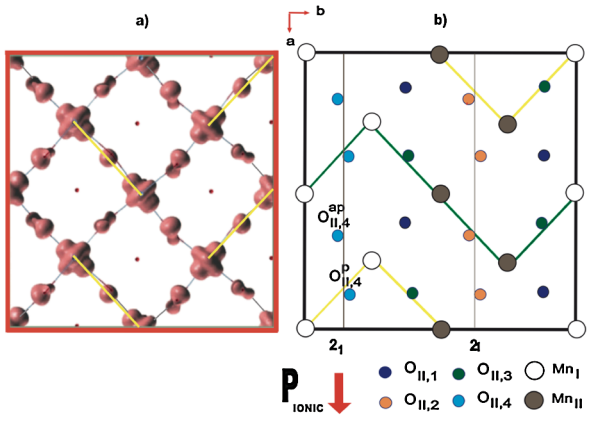

FIG. 4 (color online). (a) DFT isosurface of the e_g bands in the LT-O structure. ZP are highlighted. (b) Atomic arrangement of the LT-O MnO_2 plane. Atoms marked with the same color are structurally equivalent (i.e., linked by symmetry in the $P2_1nm$ space group). Zigzag spin chains highlighted.

ZP-like dimer, which is $\sim 0.05 \mu_B$, at variance with much larger values predicted by Hartree-Fock calculations [30,31]. Therefore, small charge-transfer effects are expected, calling for further studies focused on the O spin polarization (especially in $Pr_{1-x}Ca_xMnO_3$, $0.3 < x < 0.5$, where the ZP seems the ground state). With a noncollinear spin arrangement, we find from DFT the LT-M (Ref. [11]) to show a lower total energy (by ~ 54.3 meV/Mn) than the LT-O (Ref. [27]). This difference reduces to ~ 22.6 meV/Mn upon ionic relaxation. These energy differences are relatively small. It is remarkable that the total polarization changes only slightly upon relaxing the structures.

The calculation of the FE polarization for LT-O structure gives particularly interesting results. In the LT-O $P2_1nm$ *nonmagnetic* space group, a *nonswitchable* polarization is allowed along the *a* axis [16]. However, we here focus on the *b* axis by investigating the possibility of *magnetically switchable* multiferroicity. The 2_1 symmetry of the $P2_1nm$ space group, forbids any ionic component of P along the *b* axis: in fact, with the experimental atomic positions, $P^b_{\text{ion}} = 0$. However, when calculating the electronic contribution to P_b, a large value is obtained ($P^b_{\text{ele}} = 7.2\ \mu\text{C/cm}^2$), which should be easily experimentally detected in untwinned and high-quality crystals. To clarify the origin of P, we remark that, upon imposing the AFM-CE spin configuration, the 2_1 screw axis is no longer a symmetry operation in the *magnetic* space group, paving the way to a finite P_b. For example, the O atoms, labeled as $O_{\text{II},4}$ in Fig. 4(b), are linked by the 2_1 symmetry in the absence of magnetic ordering. However, with the CE-type spin configuration, they are alternatively bonded to Mn with parallel ($O^p_{\text{II},4}$) and with antiparallel ($O^{ap}_{\text{II},4}$) spins. They are therefore *structurally equivalent but electronically inequivalent*, as suggested by the e_g charge density plot [Fig. 4(a)]. Indeed, their inequivalency is the origin of polarization in LT-O: inversion symmetry is therefore broken by a combination of structural, BC charge and spin degrees of freedom.

In summary, we have found two different mechanisms for improper ferroelectricity in LCMO. In the first one, starting from centrosymmetric ionic positions and double-zigzag ferromagnetic spin chains, an intermediate bond-centered/site-centered polar charge distribution is achieved by means of a spin dimerization. This induces a dramatic ferroelectric response with P up to few $\mu\text{C/cm}^2$. The second mechanism, active in the bond-centered ZP-like lattice structure, induces ferroelectricity along the *b* axis, with the AFM-CE spin arrangement lifting the 2_1 symmetry and paving way to a value of P_b which is largest to date in the whole class of improper magnetic ferroelectrics. Recent electric field gradient experiments on doped manganites have also suggested the existence of ferroelectric domains in the charge ordered regime [32].

The research leading to part of these results has received funding from the European Research Council under the European Community 7th Framework Program (FP7/2007-2013)/ERC Grant Agreement No. 203523, from NanoNed and FOM. Computing time from the NCF is gratefully acknowledged.

[1] S. W. Cheong and M. Mostovoy, Nature Mater. **6**, 13 (2007).
[2] R. Ramesh and N. A. Spaldin, Nature Mater. **6**, 21 (2007).
[3] W. Eerenstein, N. D. Mathur, and J. F. Scott, Nature (London) **442**, 759 (2006).
[4] T. Kimura *et al.*, Nature (London) **426**, 55 (2003).
[5] N. Hur *et al.*, Nature (London) **429**, 392 (2004).
[6] T. Lottermoser *et al.*, Nature (London) **430**, 541 (2004).
[7] J. van den Brink and D. Khomskii, J. Phys. Condens. Matter **20**, 434217 (2008).
[8] M. Imada, A. Fujimori, and Y. Tokura, Rev. Mod. Phys. **70**, 1039 (1998).
[9] D. V. Efremov, J. van den Brink, and D. I. Khomskii, Nature Mater. **3**, 853 (2004).
[10] G. C. Milward, M. J. Calderon, and P. B. Littlewood, Nature (London) **433**, 607 (2005).
[11] P. G. Radaelli *et al.*, Phys. Rev. B **55**, 3015 (1997).
[12] E. O. Wollan and W. C. Koehler, Phys. Rev. **100**, 545 (1955).
[13] J. B. Goodenough, Phys. Rev. **100**, 564 (1955).
[14] S. Grenier *et al.*, Phys. Rev. B **69**, 134419 (2004); F. Rivadulla *et al.*, *ibid.* **66**, 174432 (2002); R. J. Goff and J. P. Attfield, *ibid.* **70**, 140404 (2004).
[15] A. Daoud-Aladine *et al.*, Phys. Rev. Lett. **89**, 097205 (2002).
[16] L. Wu *et al.*, Phys. Rev. B **76**, 174210 (2007).
[17] J. J. Betouras, G. Giovannetti, and J. van den Brink, Phys. Rev. Lett. **98**, 257602 (2007).
[18] S. Picozzi *et al.*, Phys. Rev. Lett. **99**, 227201 (2007).
[19] G. Giovannetti and J. van den Brink, Phys. Rev. Lett. **100**, 227603 (2008).
[20] C. Wang *et al.*, Phys. Rev. Lett. **99**, 177202 (2007).
[21] H. J. Xiang and M. H. Whangbo, Phys. Rev. Lett. **99**, 257203 (2007).
[22] J. P. Perdew *et al.*, Phys. Rev. Lett. **77**, 3865 (1996).
[23] V. I. Anisimov *et al.*, J. Phys. Condens. Matter **9**, 767 (1997).
[24] G. Kresse and J. Furthmüller, Phys. Rev. B **54**, 11 169 (1996).
[25] D. Hobbs, G. Kresse, and J. Hafner, Phys. Rev. B **62**, 11 556 (2000).
[26] R. D. King-Smith and D. Vanderbilt, Phys. Rev. B **47**, 1651 (1993); R. Resta, Rev. Mod. Phys. **66**, 899 (1994).
[27] E. E. Rodriguez *et al.*, Phys. Rev. B **71**, 104430 (2005).
[28] Z. Popovic and S. Satpathy, Phys. Rev. Lett. **88**, 197201 (2002).
[29] S. Yunoki *et al.*, Phys. Rev. Lett. **84**, 3714 (2000); S. Kumar and A. P. Kampf, *ibid.* **100**, 076406 (2008).
[30] C. H. Patterson, Phys. Rev. B **72**, 085125 (2005).
[31] V. Ferrari, M. Towler, and P. B. Littlewood, Phys. Rev. Lett. **91**, 227202 (2003).
[32] A. M. Lopes *et al.*, Phys. Rev. Lett. **100**, 155702 (2008).